

# Spin-resolved quantum-dot resonance fluorescence

A. Nick Vamivakas<sup>1\*†</sup>, Yong Zhao<sup>1,2\*</sup>, Chao-Yang Lu<sup>1,3</sup> and Mete Atatüre<sup>1†</sup>

**Confined spins in self-assembled semiconductor quantum dots promise to serve both as probes for studying mesoscopic physics in the solid state and as stationary qubits for quantum-information science<sup>1–7</sup>. Moreover, the excitations of self-assembled quantum dots can interact with near-infrared photons, providing an interface between stationary and ‘flying’ qubits. Here, we report the observation of spin-selective photon emission from a resonantly driven quantum-dot transition. The Mollow triplet<sup>8</sup> in the scattered photon spectrum—the hallmark of resonance fluorescence when an optical transition is driven resonantly—is presented as a natural way to spectrally isolate the photons of interest from the original driving field. We also demonstrate that the relative frequencies of the two spin-tagged photon states can be tuned independent of an applied magnetic field through the spin-selective dynamic Stark effect, induced by the same driving laser. This demonstration should be a step towards the realization of challenging tasks such as electron-spin readout, heralded single-photon generation for linear-optics quantum computing and spin-photon entanglement.**

In the realm of solid-state emitters generating flying qubits, milestone achievements so far include single-photon antibunching<sup>9,10</sup>, entangled photon-pair generation<sup>11</sup> and cavity quantum electrodynamics in the strong coupling regime<sup>12–14</sup>. A common feature in all of these studies is the incoherent pumping of the quantum-dot transitions through carrier generation in either the host matrix such as GaAs or the quasi-continuum states above the higher-lying confined states of the quantum dot. This excitation method leads to photon-emission-time jitter and spectral wandering of the quantum-dot transition larger than the transition’s linewidth. Both effects reduce the usefulness of non-resonantly generated single photons in linear-optics quantum computing algorithms<sup>15</sup>, even if the quantum dot is coupled to a cavity. In an attempt to both address this previous shortcoming and provide spectrally selective access to the quantum-dot electronic transitions, increasing attention has turned to resonant optical excitation. So far, resonant optical addressing of quantum dots has relied predominantly on a remarkably powerful laser-based spectroscopy technique: differential transmission<sup>16</sup>. Although differential transmission has enabled progress in spin-selective excitation of quantum dots, access to the scattered photons correlated with the quantum-dot spin has proven elusive. Recently, differential transmission and, independently, cavity-assisted temporal correlation measurements have shown clear signatures of dressed-state formation under strong laser light excitation on neutral quantum dots<sup>17–21</sup>. Noting all successful quantum-information science (QIS) implementations on well-developed qubit candidates, such as trapped ions, have relied on spin-selective resonance scattering<sup>22</sup>, it is clear that an immediate goal for quantum dots is the observation of

the full resonance fluorescence spectrum carrying the desired spin-qubit information.

Coupling two states of a quantum system by a monochromatic laser results in scattered photons with distinct spectral and coherence properties that may be tuned as the properties of the laser (for example, power, frequency and polarization) are varied. Barring any dephasing mechanisms, when the effective Rabi frequency is much less than the spontaneous emission rate, the interference between the scattered photons and the laser field forms the basis of the above-mentioned differential-transmission technique. When the effective Rabi frequency is larger than the spontaneous emission rate, the electronic states are dressed (see Fig. 1a, inset)<sup>23</sup>. The spectrum of the photons scattered in this limit exhibits a multi-Lorentzian structure known as the Mollow triplet<sup>8</sup>—first observed on atomic sodium in 1975 (ref. 24) and as recent as 2007 on a single molecule<sup>25</sup>. The central frequencies for these transitions are:

$$\begin{aligned} \nu_{\text{red}} &= \nu_0 + \Delta - \Omega; & \nu_{\text{central}} &= \nu_0 + \Delta; \\ \nu_{\text{blue}} &= \nu_0 + \Delta + \Omega, \end{aligned} \quad (1)$$

and the linewidth of each detuned sideband is  $(3/2)\gamma_{\text{sp}}$ . Here,  $\nu_0$  is the bare quantum-dot  $X^{-1}$  transition frequency,  $\Delta$  is the laser frequency detuning from  $\nu_0$  (negative for red-detuning) and  $\Omega = \sqrt{\Delta^2 + \Omega_b^2}$  ( $\Omega_b$ ) is the effective (bare) Rabi frequency.

We start by presenting the observation of the Mollow triplet in the resonance fluorescence spectrum from a single-quantum-dot transition and then proceed to link this with the quantum-dot spin. Figure 1a shows  $X^{-1}$  resonance fluorescence spectra on a linear–log scale for a range of laser powers (no external magnetic field). The laser is resonant with the doubly degenerate bare  $X^{-1}$  quantum-dot transition frequency. For laser powers above 216 nW, two equal-weight sidebands emerge, which, together with the central feature, constitute the Mollow triplet. The sharp peak in the central feature is residual laser background (see Supplementary Information, Fig. S2). Peak-to-peak sideband splittings determined from this data are plotted in Fig. 1b against the square root of the laser power. In the strong excitation regime ( $\Omega_b \geq \gamma_{\text{sp}}$ ), the linear fit confirms the dependence of the sideband splitting on the square root of the laser power.

The observation of the Mollow triplet from a quantum dot should not come as a surprise; however, the measured sideband linewidths are intriguing. Figure 1c shows a linear–linear zoom-in on the Mollow sidebands for a laser power of 1.852  $\mu\text{W}$  ( $\Omega_b \approx 8\gamma_{\text{sp}}$ ). When fitted with the resonance fluorescence spectrum (see Supplementary Information, Discussion), a transition linewidth of 343 ( $\pm 39$ ) MHz per sideband is extracted, in close agreement with the pure spontaneous emission rate of 227 ( $\pm 7$ ) MHz obtained from photon-correlation measurements at an excitation power well below saturation. The linewidth places an upper bound of

<sup>1</sup>Cavendish Laboratory, University of Cambridge, JJ Thomson Avenue, Cambridge CB3 0HE, UK, <sup>2</sup>Physikalisches Institut, Ruprecht-Karls-Universität Heidelberg, Philosophenweg 12, 69120 Heidelberg, Germany, <sup>3</sup>HFNL & Department of Modern Physics, University of Science and Technology of China, Hefei, 230026, China. \*These authors contributed equally to this work. †e-mail: anv21@cam.ac.uk; ma424@cam.ac.uk.

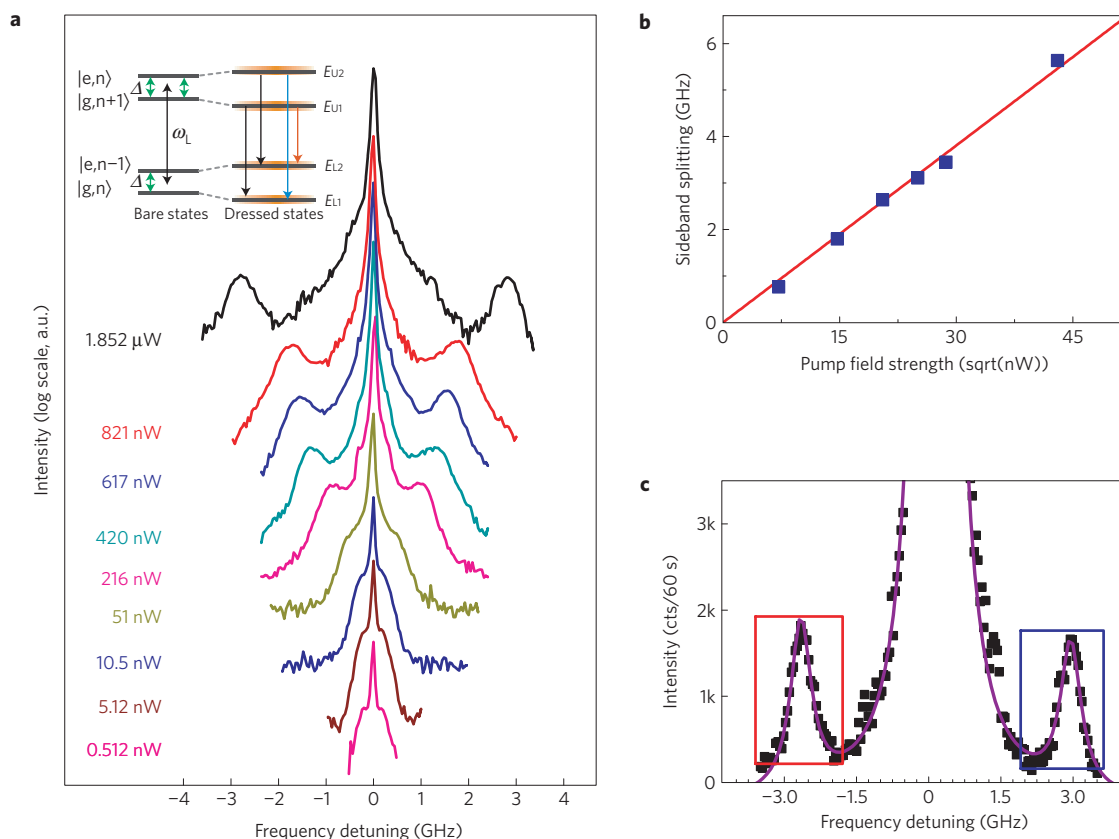


**Figure 1 | Power-dependent resonance fluorescence.** **a**, Evolution of the Mollow triplet spectrum as the resonant laser power is increased from 0.512 nW ( $\Omega_b \approx 0.13\gamma_{sp}$ ) to 1.852  $\mu$ W ( $\Omega_b \approx 8\gamma_{sp}$ ) under zero magnetic field. The intensity of the spectrum is plotted on a logarithmic scale. Each data point is recorded for 60 s. The inset illustrates the Jaynes-Cummings ladder structure for the dressed two-level system in a strong laser field that is red-detuned by  $\Delta$  from the resonance. Four possible transitions are indicated, two of them are frequency degenerate. **b**, Extracted sideband splitting as a function of pump field strength (that is, the square root of the pump power) on a linear scale. The data points exhibit a linear relationship between the square root of the laser power and the sideband splitting (determined by the Rabi frequency). **c**, Zoom-in plot of the 1.852  $\mu$ W fluorescence spectrum sidebands with a linear intensity scale. The rectangles highlight the sidebands from which we extract a transition linewidth of 343 ( $\pm 39$ ) MHz.

81 MHz on further fast dephasing mechanisms as determined from  $\gamma_{total} = \gamma_{sp} + 2\gamma_{dephasing}$ . This suggests that emission from the triplet sidebands of the dressed quantum-dot transition may be at the transform limit. Further first- and second-order coherence experiments on the individual sidebands are necessary to determine the deviation from the Fourier-transform limit for the sideband photons.

In addition to the laser power, the sideband spectrum may also be tuned by the laser frequency. In Fig. 2a, the measured  $X^{-1}$  resonance fluorescence spectra, driven by 1.852  $\mu$ W laser power ( $\Omega_b \approx 8\gamma_{sp}$ ), are plotted for a set of laser-frequency detunings ( $\Delta$ ). For comparison, Fig. 2b shows equation (1) as a function of the laser frequency detuning at fixed laser power. Measuring the spectral separation of the red sideband (when the laser is red-detuned by 2.48 GHz) from the blue sideband (when the laser is blue-detuned by 3.32 GHz) it is possible to achieve photon emission across a frequency band of  $\sim 14$  GHz. This is 40 times larger than the 227 MHz spontaneous emission rate, and is by no means an upper limit, but can be further increased by laser power and detuning. To relate this range to other tuning mechanisms, we emphasize that 16 GHz is the range obtainable through d.c. Stark shift of the  $X^{-1}$  transition throughout the whole single-electron charging plateau<sup>5</sup>. Alternatively, this is the same frequency shift that each of the two degenerate  $X^{-1}$  transitions experiences under an applied magnetic field of 1 T (ref. 26). The sideband splittings extracted from the data set of Fig. 2a are plotted in Fig. 2c as a function of laser detuning. The red fit curve with the functional form of  $2\sqrt{\Delta^2 + \Omega_b^2}$  is used to

determine a bare Rabi frequency of  $2.76 \pm 0.2$  GHz. From this value, we determine a dipole moment of  $27.8 \pm 0.2$  Debye, in agreement with our differential-transmission measurements.

The final part of this letter is on optical access to a quantum-dot spin, through resonance fluorescence, where a finite magnetic field splits the electronic spin ground states, lifting the  $X^{-1}$  spin degeneracy. A reproduction of Fig. 2b under finite magnetic field and accounting for spin is presented in Fig. 3a. The two dressed Zeeman-split sidebands (the blue and red solid lines) are directly correlated to the spin state of the electron and their frequency splitting is controlled by laser detuning beyond that manifested by the magnetic field. In what follows, all frequencies are referenced to the zero-magnetic-field quantum-dot  $X^{-1}$  resonance. First, a 50 mT external magnetic field is applied in the Faraday configuration. In Fig. 3b, the fluorescence spectrum of the blue-detuned sideband (the blue rectangle in Fig. 3a) is plotted for laser detunings of 1.75, 1.25 and 0 GHz, from left to right. By varying the laser detuning, at constant power, the Zeeman splitting of the transitions induced by the magnetic field can be altered (Fig. 3b, panels 1 and 2) and even cancelled (Fig. 3b, panel 3).

What we have demonstrated is a combined outcome of the Zeeman and dynamic Stark effect<sup>6,18,27</sup>, which enables us to tune independently the energy splitting of the ground and excited states. For InGaAs quantum dots, the electron and hole  $g$ -factors are known to be around  $-0.6$  and  $1.4$  (ref. 26). Therefore, the ground- and excited-state manifolds respond differently to the external magnetic field. The dynamic Stark effect, however,







